

# Refined Multifractal Cross-Correlation Analysis

Paweł Oświęcimka,<sup>1,\*</sup> Stanisław Drożdż,<sup>1,2</sup> Marcin Forczek,<sup>1</sup> Stanisław Jadach,<sup>1</sup> and Jarosław Kwapien<sup>1</sup>

<sup>1</sup>*Institute of Nuclear Physics, Polish Academy of Sciences, Kraków, Poland.*

<sup>2</sup>*Faculty of Physics, Mathematics and Computer Science,  
Cracow University of Technology, Kraków, Poland.*

(Dated: August 29, 2013)

We propose a modified algorithm - Multifractal Cross-Correlation Analysis (MFCCA) - that is able to consistently identify and quantify multifractal cross-correlations between two time series. Our motivation for introducing this algorithm is that the already existing methods like MF-DXA have serious limitations for most of the signals describing complex natural processes. The principal component of the related improvement is proper incorporation of the sign of fluctuations. We present a broad analysis of the model fractal stochastic processes as well as of the real-world signals and show that MFCCA is a robust tool and allows a reliable quantification of the cross-correlative structure of analyzed processes. We, in particular, analyze a relation between the generalized Hurst exponent and the MFCCA parameter  $\lambda_q$ . This relation provides information about the character of potential multifractality in cross-correlations of the processes under study and thus enables selective insight into their dynamics. Using also an example of financial time series from the stock market we show that waiting times and price increments of the companies are multifractally cross-correlated but only for relatively large fluctuations, whereas the small ones could be considered mutually independent.

PACS numbers: 05.10.-a, 05.45.Df, 05.45.Tp

## I. INTRODUCTION

Analysis of time series with nonlinear long-range correlations is often grounded on a study of their multifractal structure [1–3]. Existing algorithms used in such an analysis allow for determining generalized fractal dimensions or Hölder exponents based either on statistical properties of time series [4, 5] or on time-frequency information [6, 7]. Because of implementation simplicity and their utility, these algorithms have already been applied to characterize correlation structure of data in various areas of science like physics [8, 9], biology [10–12], chemistry [13, 14], economics [15–17] and music [18, 19]. In recent years, algorithms designed for investigation of fractal cross-correlations were also proposed [20, 21]. Detrended Cross-Correlation Analysis (DCCA) is a simple generalization of the fractal auto-correlation (DFA) [22] on the case of fractally cross-correlated signals. In that case, the cross-correlation scaling exponent  $\lambda$  can be obtained. However, literature still lacks comprehensive interpretation of this quantity.

Subsequently, the multifractal variant (MF-DXA) of the DCCA method was proposed [23]. However, as our analyses show (see section II and III B), this method and its simple modifications, based on taking modulus [24–26] of the cross-covariance function in order to get rid of the negative signs, have serious limitations since such situations often happen in realistic cases. Our motivation therefore is to elaborate an algorithm that we call Multifractal Cross-Correlation Analysis (MFCCA), such that it properly takes care of the sign already in its definition.

The proposed method allows us to calculate the spectrum of  $\lambda_q$  exponents which characterize multifractal properties of the cross-covariance. However, unlike the method proposed earlier, in our procedure, the scaling properties of the  $q$ th order cross-covariance function are estimated with respect of the original sign of cross-covariance. This procedure makes the method both more sensitive to cross-correlation structure and free from limitations of other algorithms. It also turns out that the proposed method is a more natural generalization of the monofractal DCCA than is MF-DXA. The robustness of our algorithm makes it applicable for different data types in various fields of science.

## II. DESCRIPTION OF THE MFCCA ALGORITHM

Multifractal Cross-Correlation Analysis consists of several steps which are described in detail below. As it was mentioned above, MFCCA has been developed based on the DCCA procedure [20], therefore the initial steps are the same.

Consider two time series  $x_i, y_i$  where  $i = 1, 2, \dots, N$ . At first, the signal profile has to be calculated for each of them:

$$X(j) = \sum_{i=1}^j [x_i - \langle x \rangle], \quad Y(j) = \sum_{i=1}^j [y_i - \langle y \rangle]. \quad (1)$$

Here,  $\langle \rangle$  denotes averaging over entire time series. Then, both signal profiles are divided into  $M_s = N/s$  disjoint segments  $\nu$  of length  $s$ . For each box  $\nu$ , the assumed trend is estimated by fitting a polynomial of order  $m$  ( $P_{X,\nu}^{(m)}$  for  $X$  and  $P_{Y,\nu}^{(m)}$  for  $Y$ ). Based on our own experience [7], as optimal we use a polynomial of order  $m = 2$

---

\*Electronic address: pawel.oswiecimka@ifj.edu.pl

throughout this paper but the proposed procedure is not restricted to this particular order. Next, the trend is subtracted from the data and the detrended cross-covariance within each box is calculated:

$$F_{xy}^2(\nu, s) = \frac{1}{s} \sum_{k=1}^s \{ (X((\nu-1)s+k) - P_{X,\nu}^{(m)}(k)) \times (Y((\nu-1)s+k) - P_{Y,\nu}^{(m)}(k)) \} \quad (2)$$

In contrast to the detrended variance calculated in the MF DFA procedure [4],  $F_{xy}^2(\nu, s)$  can take both positive and negative values (for an example see Sec. III C Fig.9). Therefore, investigation of scaling properties of small and large fluctuations separately should take into account also the sign of  $F_{xy}^2(\nu, s)$ . Accordingly, the  $q$ th order covariance function is determined by the following equation:

$$F_{xy}^q(s) = \frac{1}{M_s} \sum_{\nu=1}^{M_s} \text{sign}(F_{xy}^2(\nu, s)) |F_{xy}^2(\nu, s)|^{q/2} \quad (3)$$

where  $\text{sign}(F_{xy}^2(\nu, s))$  denotes sign of the  $F_{xy}^2(\nu, s)$  function. The  $q$  parameter can take any real number except zero. However, for  $q = 0$  the logarithmic version of Eq. (3) can be employed [4]:

$$F_{xy}^0(s) = \frac{1}{M_s} \sum_{\nu=1}^{M_s} \text{sign}(F_{xy}^2(\nu, s)) \ln |F_{xy}^2(\nu, s)| \quad (4)$$

As we can see in Eq. (3), for negative values of  $q$ , small values of covariance function  $F_{xy}^2(\nu, s)$  are amplified, while for large  $q > 0$ , its large values dominate. Moreover, the formula of calculating  $F_{xy}^q(s)$  respects the genuine signs of the amplified (or suppressed) fluctuations of detrended cross-correlations function. This procedure allows to avoid numerical errors associated with the power (with rational and even exponents) of negative fluctuations. The above described steps of MFCCA should be repeated for different scales  $s$ . If the so-obtained function  $F_{xy}^q(s)$  does not develop scaling, by for instance fluctuating around zero, there is no fractal cross-correlation between the analyzed series for the considered value of  $q$ . Multifractal cross-correlation is expected to manifest itself in the power-law dependence of  $F_{xy}^q(s)$  ( if the  $q$ th order covariance function is negative for every  $s$ , we may take  $F_{xy}^q(s) \rightarrow -F_{xy}^q(s)$  [20]) and the following relation is fulfilled:

$$F_{xy}^q(s)^{1/q} = F_{xy}(q, s) \sim s^{\lambda_q} \quad (5)$$

(or  $\exp(F_{xy}^0(s)) = F_{xy}(0, s) \sim s^{\lambda_0}$  for  $q = 0$ ) where  $\lambda_q$  is an exponent that quantitatively characterizes fractal properties of the cross-covariance. For the monofractal cross-correlation, the exponents  $\lambda_q$  are independent of  $q$  and equal to  $\lambda$  as obtained from the DCCA method. In the case of multifractal cross-correlation, however,  $\lambda_q$  varies with  $q$ , whereas  $\lambda$  is retrieved for  $q = 2$ . The minimum and maximum scales ( $s_{min}$  and  $s_{max}$ , respectively) depend on the length  $N$  of time series under study. In

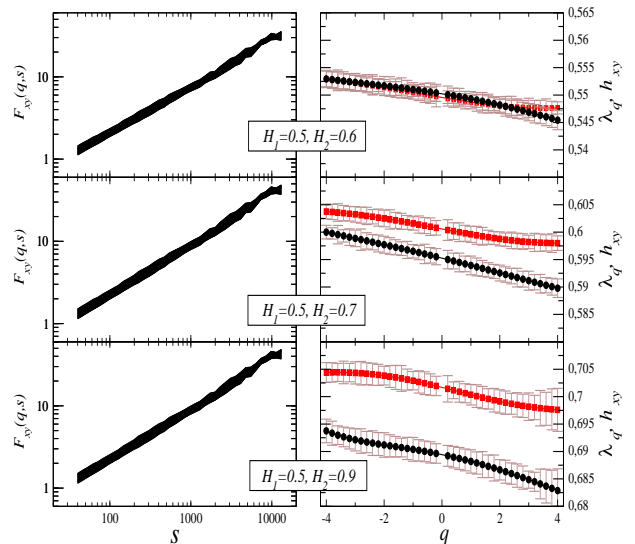


FIG. 1: Cross-correlation characteristics obtained by averaging over a sample of 20 independently generated pairs of ARFIMA processes for three different combinations of  $H_1$  and  $H_2$  parameters. Left panels: the family of the  $F_{xy}(q, s)$  functions. The lowest and the highest lines on each panel refers to  $q = -4$  and  $q = 4$ , respectively. Right panels: circles (black) refer to  $\lambda_q$  and squares (red) refer to the average of the generalized Hurst exponents  $h_{xy}(q)$ . Error bars indicate standard deviation calculated from 20 independent realizations of the corresponding process.

practice, it is reasonable to take  $s_{max} < N/5$ . Moreover, in order to avoid divergent moments due to fat tails in the distribution of fluctuations, we restrict  $q$  to  $(-4, 4)$  with a step 0.2.

### III. ANALYSIS OF EXEMPLARY MODELS AND STOCK MARKET DATA

In order to verify the usefulness of MFCCA algorithm, we test it by using both artificially generated cross-correlated time series and real-world signals. In the case of computer-generated signals, results for each process are averaged over its 20 independent realizations.

#### A. ARFIMA processes

We start our study from an analysis of the well-known ARFIMA processes [27], which are examples of monofractal, long-range correlated signals. In Ref. [20], such processes were used to show usefulness of the DCCA algorithm. Our goal is to show the cross-correlation structure of the above-mentioned processes more completely. To generate a pair  $(x_i, y_i)$  of the cross-correlated ARFIMA processes, we use the following equations:

$$x_i = \sum_{j=1}^{\infty} a_j(d_x) x_{i-j} + \epsilon_i \quad (6)$$

$$y_i = \sum_{j=1}^{\infty} a_j(d_y) y_{i-j} + \epsilon_i \quad (7)$$

where  $d_x$  and  $d_y$  are parameters characterizing linear long-range autocorrelations of the time series. These quantities can be related to the Hurst exponents [22] by the relation  $H = 1/2 + d_{x(y)}$ , ( $-1/2 < d_{x(y)} < 1/2$ ). Positively correlated (persistent) time series are characterized by  $H > 0.5$  whereas negative autocorrelation (antipersistent signal) is quantified by  $H < 0.5$ ;  $H=0.5$  means no linear autocorrelation. The quantity  $a_j(d_{x(y)})$  is called weight and it is defined by  $a_j(d_{x(y)}) \equiv \Gamma(j - d_{x(y)}) / [\Gamma(-d_{x(y)})\Gamma(1 + j)]$ , where  $\Gamma()$  stands for Gamma function.  $\epsilon_i$  is an i.i.d. Gaussian random variable. The processes  $x_i$  and  $y_i$  are cross-correlated, because the same noise component  $\epsilon_i$  is used in both Eq.(6) and Eq.(7). We generate three pairs of cross-correlated signals: ( $H_1=0.5$ ,  $H_2=0.6$ ), ( $H_1=0.5$ ,  $H_2=0.7$ ), and ( $H_1=0.5$ ,  $H_2=0.9$ ), where  $H_1$  and  $H_2$  characterize long-range autocorrelation of the first and the second time series, respectively. In order to obtain statistically significant results, we generate time series of length  $N = 100,000$  points each.

In the left panels of Fig. 1, we present the calculated  $F_{xy}(q, s)$  for all the considered pairs of signals. Each line corresponds to a different value of  $q$ . As it can be seen, in all the cases,  $F_{xy}(q, s)$  is a power function of scale  $s$ . This indicates the fractal nature of the cross-correlations. Moreover, for all types of signals, the functions  $F_{xy}(q, s)$  are almost parallel to each other implying largely homogeneous character of the corresponding cross-correlations. Indeed, as shown in the right panels of the Fig. 1, the difference between the extreme values of  $\lambda_q$  expressed by  $\Delta\lambda_q = \max(\lambda_q) - \min(\lambda_q)$  is approximately 0.005, 0.007, and 0.011 for the top, middle, and the bottom panel, respectively. These narrow ranges of  $\lambda_q$  indicate that the ARFIMA processes reveal correlations that are monofractal regardless of the types of linear autocorrelation of signals.

In literature, the estimated fractal cross-correlations are often related to the fractal properties of the signals themselves [20, 28, 29]. Therefore, in Fig. 1, we also show the average of the generalized Hurst exponents [4]:

$$h_{xy}(q) = (h_x(q) + h_y(q))/2, \quad (8)$$

where  $h_x(q)$  and  $h_y(q)$  refer to fractal properties of individual time series, respectively and, for  $q = 2$ , they correspond to the Hurst exponent  $H$ . It is worth noticing that relation between  $\lambda_q$  and  $h_{xy}(q)$  functions depends on temporal organization of the signals as determined by their Hurst exponents. For two signals whose Hurst exponents  $H$  are alike, their multifractal cross-correlation characteristics described by  $\lambda_q$  and  $h_{xy}(q)$  are almost identical whereas for time series with more pronounced differences of autocorrelation (different Hurst exponent  $H$ ) the divergence between  $\lambda_q$  and  $h_{xy}(q)$  becomes more sizeable.

This result means that, in the case of the ARFIMA processes, the relation  $\lambda \approx (h_x(2) + h_y(2))/2$  introduced in Ref. [20] applies only to a case when differences between  $h_x$  and  $h_y$  are negligible.

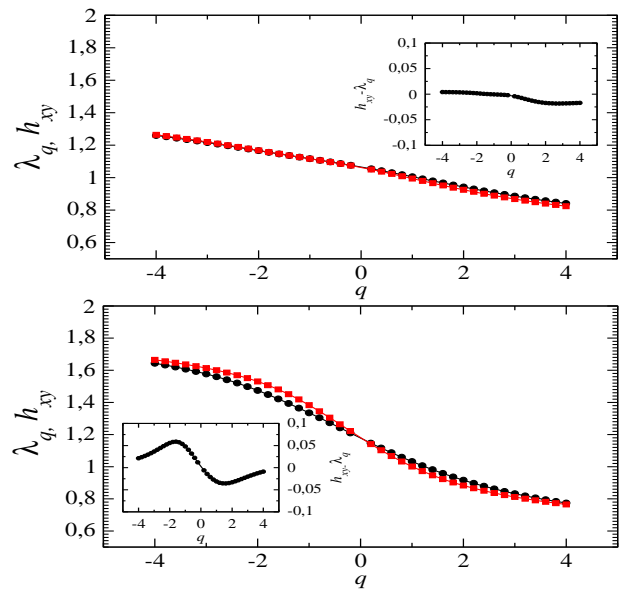


FIG. 2: Cross-correlation characteristics calculated for two pairs of MSM time series corresponding to  $m_{01} = 1.2$ ,  $m_{02} = 1.35$  (top) and  $m_{01} = 1.2$ ,  $m_{02} = 1.6$  (bottom), respectively. Circles (black) in the main plots refer to  $\lambda_q$  and squares (red) refer to the average of generalized Hurst exponents  $h_{xy}(q)$ . Insets present the differences between  $\lambda_q$  and  $h_{xy}$  function.

## B. Markov-switching multifractal model

As an example of multifractal process, we consider the Markov-switching multifractal model (MSM) [30]. MSM is an iterative model, which is able to replicate hierarchical, multiplicative structure of real data and, thus, insures multifractal properties of the generated time series. Because of its properties, MSM is commonly used in finance, where multifractality of price fluctuations is one of the main stylized facts [31, 32]. Below, we present the main stages of the model's construction.

In MSM, evolution of an observable  $r_t$  in time  $t$  is modeled by the formula [31]:

$$r_t = \sigma_t \cdot u_t, \quad (9)$$

where  $u_t$  stands for a Gaussian random variable and  $\sigma_t$  (multifractal process) stands for the instantaneous volatility component. The volatility  $\sigma_t$  is a product of  $k$  multipliers  $M_1(t), M_2(t), \dots, M_k(t)$  such that

$$\sigma_t^2 = \sigma^2 \prod_{i=1}^k M_i(t), \quad (10)$$

where  $\sigma^2$  is a constant factor. A popular version of the model assumes that the multipliers  $M_i(t)$  are drawn from the binomial or from the log-normal distribution. Here, we use the binomial one with  $M_i(t) \sim \{m_0, 2 - m_0\}$ , ( $1 \leq m_0 < 2$ ). Any change of a multiplier in the hierarchical structure of volatility is determined by the transi-

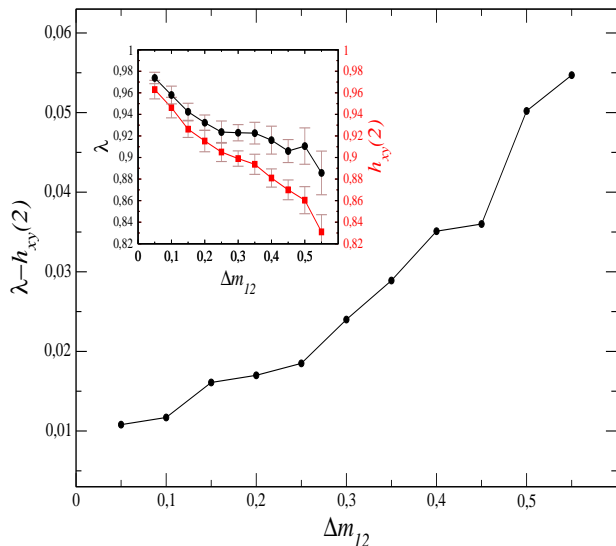


FIG. 3: Inset: the average of  $\lambda_2 = \lambda$  and average of  $h_{xy}(2)$  as a function of  $\Delta m_{12} = m_{02} - m_{01}$ . Circles (black) and squares (red) correspond to the  $\lambda$  and  $h_{xy}(2)$ , respectively. Error bars indicate standard deviation calculated from 20 independent realizations of the corresponding process. Main: the difference of the average of  $\lambda$  and the average of  $h_{xy}(2)$  as a function of  $\Delta m_{12}$ .

tion probabilities [30]:

$$\gamma_i = 1 - (1 - \gamma_k)^{b^{i-k}}, \quad i = 1, 2, \dots, k. \quad (11)$$

Thus, a multiplier  $M_i(t)$  is renewed with probability  $\gamma_i$  and remains unchanged with probability  $1 - \gamma_i$ . The parameter  $\gamma_k$  is taken from the range  $(0, 1)$ , and  $b \in (1, \infty)$ . We impose  $\gamma_k = 0.5$  and  $b = 2$ , which leads to the relation:

$$\gamma_i = 1 - (0.5)^{2^{i-k}}, \quad i = 1, 2, \dots, k. \quad (12)$$

Thus, for the initial stages of the cascade, a renewal of the multipliers  $M_i(t)$  occurs with relatively small probability, while the largest  $\gamma_i = 0.5$  appears for  $i = k$ . For the purpose of this analysis, we generate a set of multifractal time series  $(\sigma_t)$  of length 131,072 points each. However, in all realizations of the model, we conserve the hierarchical structure of the multipliers, since the renewals of  $M_i(t)$  appear for the same  $i$  and  $t$  in each generated series. This procedure insures cross-correlations between series with different  $m_0$ .

In Fig. 2, we present sample results of MFCCA obtained for two pairs of MSM series with the parameters  $m_{01} = 1.2$  and  $m_{02} = 1.35$  for the top panel and  $m_{01} = 1.2$  and  $m_{02} = 1.6$  for the bottom one. It is easy to notice that, in both cases,  $\lambda_q$  is a decreasing function of  $q$ , which is a hallmark of multifractality. Moreover, the rate of decrease of  $\lambda_q$  depends on the values of multipliers. For the first pair of signals (with  $m_{02} = 1.35$ ), the exponents  $\lambda_q$  are contained in the range  $(0.81, 1.25)$  while for the signals with the larger values of  $m_{02}$ ,  $0.75 \leq \lambda_q \leq 1.7$ .

In the same Fig. 2, we also show the average of the generalized Hurst exponents calculated for each time series independently (black circles).

Interestingly, for the signals with a relatively small difference  $\Delta m_{12} = m_{02} - m_{01}$  - in other words, for similar multifractals -  $\lambda_q$  approximately equals the average of  $h_x(q)$  and  $h_y(q)$ . Tiny difference between  $h_{xy}(q)$  and  $\lambda_q$  is here visible only for  $q > 0$ . This effect is depicted more quantitatively in the insets of Fig. 2, where  $h_{xy}(q) - \lambda_q$  is presented as a function of  $q$ . The maximum deviation from zero can be seen for  $q = 2.2$ , reaching a value of 0.02. For the second pair of signals, the difference  $h_{xy}(q) - \lambda_q$  is more pronounced and concerns both negative and positive  $q$ 's. In this case, the largest difference of  $h_{xy}(q)$  and  $\lambda_q$  is for  $q = -2$  and equals 0.07.

To have some insight into the relation between  $\lambda_q$  and  $h_{xy}(q)$ , we perform a systematic MFCCA study for the set of time series pairs, such that one of them is generated with  $m_{01} = 0.1$  and the other one with  $m_{02}$  from the range  $(0.05, 0.9)$  (the step is 0.05). However, the multifractal characteristics were possible to estimate only for  $\Delta m_{12} < 0.6$ . In the case of  $\Delta m_{12} > 0.6$ ,  $F_{xy}^q$  takes both positive and negative values and Eq.(5) is not satisfied. At first, we focus on the relationship between  $\lambda_2 = \lambda$  and the average Hurst exponent  $h_{xy}(2)$ . In the inset of Fig. 3, we present these quantities as a function of  $\Delta m_{12}$ . It is clearly visible that both these quantities are monotonically decreasing and they take approximately the same values for small  $\Delta m_{12}$ . However, for  $\Delta m_{12} > 0.25$ ,  $\lambda(\Delta m_{12})$  decreases slower than the Hurst index (thus  $\lambda > H$ ) and the statistics diverge. To highlight this result, we calculate also the difference between these two quantities which is shown in Fig.3. As one can see,  $\lambda - h_{xy}(2)$  is increasing function of  $\Delta m_{12}$ . This result indicates that difference between  $\lambda$  and the average of the Hurst exponents becomes larger for two time series whose multifractal characteristics depart more from each other, while the opposite is observed when these characteristics are alike, which at the same time results in stronger cross-correlations.

To better understand this effect, we analyze a covariance function  $F_{xy}(2, s) \sim s^\lambda$  and an expression based on fluctuation functions [4]:  $\sqrt{F_{xx}(2, s)F_{yy}(2, s)} \sim s^{\frac{h_x(2)+h_y(2)}{2}} = s^{h_{xy}(2)}$ . In Fig. 4, we show these functions calculated for different values of  $\Delta m_{12}$ . It is easy to notice that the presented functions are almost identical to each other for small  $\Delta m_{12}$ . However, the larger  $\Delta m_{12}$  is, the more visible is a departure between the analyzed statistics. In all cases, the values of  $F_{xy}(2, s)$  are at most equal to  $\sqrt{F_{xx}(2, s)F_{yy}(2, s)}$  and estimated  $\lambda$  is larger than  $h_{xy}(2)$ . These numerical results are in accord with the following relation:

$$F_{xy}(2, s) \leq \sqrt{F_{xx}(2, s)F_{yy}(2, s)}, \quad (13)$$

which straightforwardly results from the definitions of these quantities considered in terms of the scalar products of vectors formed from the underlying time se-

ries [24]. In order to more clearly see the relationship between  $\lambda$  and  $h_{xy}(2)$ , we can reformulate Eq. (13) in the case when the relations  $F_{xy}(2, s) = a_{xy}s^\lambda$ ,  $F_{xx}(2, s) = a_x s^{h_x(2)}$ , and  $F_{yy}(2, s) = a_y s^{h_y(2)}$  apply, to obtain:

$$a_{xy}s^\lambda \leq (a_x a_y)^{1/2} s^{\frac{h_x(2)+h_y(2)}{2}}. \quad (14)$$

This leads to:

$$\lambda \leq \log_s \left( \frac{(a_x a_y)^{1/2}}{a_{xy}} \right) + \frac{h_x(2) + h_y(2)}{2}. \quad (15)$$

For two identical time series, the equality in Eq. (13) holds leading to obvious  $\lambda = \frac{h_x(2)+h_y(2)}{2}$ . In general, however,

$$A_r = \frac{(a_x a_y)^{1/2}}{a_{xy}} \neq 1, \quad (16)$$

and thus a difference between  $\lambda$  and  $h_{xy}(2)$  in either direction is allowed or even forced, depending on a sign of  $\log_s(A_r)$ . For negative values of this quantity,  $\lambda$  has to be smaller than  $h_{xy}(2)$ , while for positive values it can become larger. An example demonstrating the rate of changes of  $\log(A_r)$  as a function of  $\Delta m_{12}$  for  $q = 2$  is shown in Fig. 5. In this case,  $\log(A_r)$  is positive and quickly increases with  $\Delta m_{12}$ , thus with the degree of dissimilarity between the two series. The related dependencies are even more involved and appear to strongly vary with the parameter  $q$  as it is more systematically shown in Fig. 6. The  $\log(A_r)$  is seen to be positive for  $q \geq 0$  with an increasing value at maximum with increasing  $\Delta m_{12}$ , and a larger amplitude of changes with increasing  $q$ . Similar, but reversed in sign and with an even larger amplitude of changes, is the situation for  $q \leq 0$ . These results nicely coincide - and thus point to their origin - with those presented in Fig. 2, where  $\lambda_q$  is larger than  $h_{xy}(q)$  for positive values of  $q$  and smaller for negative ones. Even the maxima of these differences occur for those values of  $q$ , where they are seen in Fig. 6 and they are larger on the negative side of  $q$ . Of course, they are also larger for larger  $\Delta m_{12}$ .

The difference between  $\lambda_q$  and  $h_{xy}(q)$  has its reflection - also consistent with the findings presented in Figs. 2 and 6 - in another popular multifractal measure, namely in the range of scaling exponents. In Fig. 7, we display  $\Delta\lambda_q$  as a function of  $\Delta m_{12}$  for the two ranges of  $q$ :  $-2 \leq q \leq 2$  and  $-4 \leq q \leq 4$ . For comparison, in the same Figure, we show  $\Delta h_{xy} = \max(h_{xy}) - \min(h_{xy})$  calculated for the same ranges of  $q$ . The  $\Delta h_{xy}(q)$  and  $\Delta\lambda_q$  are seen to be monotonically increasing functions of  $\Delta m_{12}$  in all the cases. However, for  $-4 \leq q \leq 4$  these characteristics are almost the same, while for  $-2 \leq q \leq 2$  the difference between  $\Delta h_{xy}$  and  $\Delta\lambda_q$  systematically increases with  $\Delta m_{12}$ . This suggests that for relatively large values of  $|q|$  (magnifying the largest and the smallest fluctuations of instantaneous volatility components) the fractal character of the considered processes is similar which may

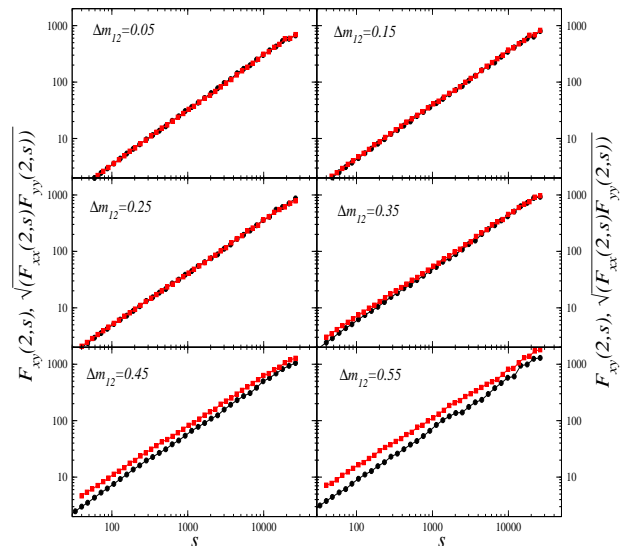


FIG. 4: Comparison of covariance function  $F_{xy}(2, s)$  (circle) with its equivalent  $\sqrt{F_{xx}(2, s)F_{yy}(2, s)}$  (squares) derived from the variance functions of individual MSM time series. The slope of this functions refers to  $\lambda_2$  and  $h_{xy}(2)$ , respectively.

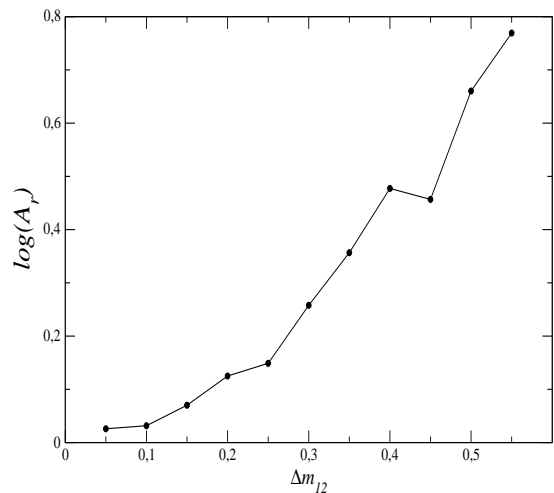


FIG. 5: Plot of  $\log(A_r)$ , calculated for  $q = 2$ , as a function of similarity parameter  $\Delta m_{12}$  of MSM time series.

reflect the effect of preserving the same hierarchical structure of multipliers for all generated multifractals, where only relative changes of volatility are possible. The above results thus indicate that the difference between  $h_{xy}(q)$  and  $\lambda_q$  is to be considered an important ingredient of measure of the fractal cross-correlation between two time series.

In the last stage of our study of MSM, we analyze output of MFCCA if one time series of a pair is gradually being shifted in time with respect to the other one. Then the correlations, especially their fractal character, should undergo weakening. This test is aimed at further verifying performance of the algorithm. As an input, we



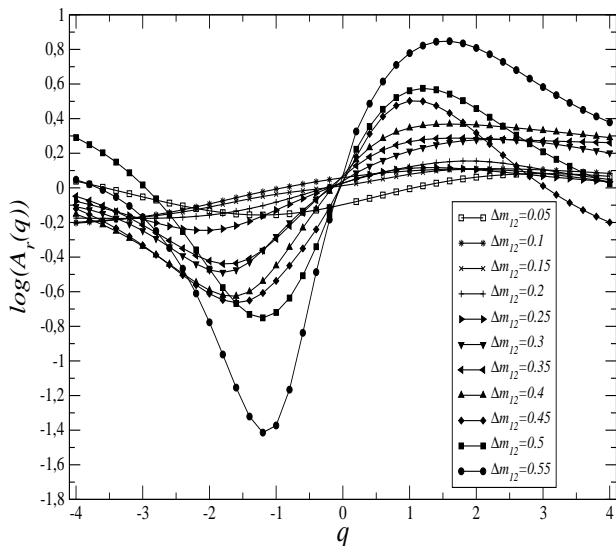


FIG. 6: Plot of  $\log(A_r)$  as a function of parameter  $q$ . Each line corresponds to different degree of similarity of MSM time series  $\Delta m_{12}$ .

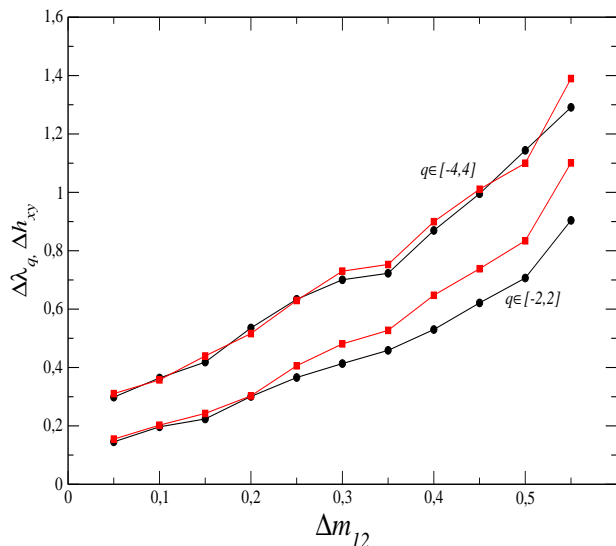


FIG. 7: Cross-correlation characteristics  $\Delta\lambda_q$  (circles) and  $\Delta h_{xy}$  (squares) as a function of multiplier difference  $\Delta m_{12} = m_{02} - m_{01}$  calculated for two ranges of  $q$  parameter.

use a time series with  $m_0 = 1.2$  and the same one, but shifted by a certain number of points. We notice that the larger is the relative shift between the time series, the shorter is the scaling range of  $F_{xy}$ . However, in all cases, the estimated  $\lambda$  is equal to the generalized Hurst exponent calculated for a single series. This shortening of the range of scaling is not symmetric from both sides of the scale range, but gradually arrives entirely from the small scale side. The shift dependence of the lower bound of the scaling regime that can be used to determine  $\lambda_q$  is shown in Fig. 8. As expected, lifting of this lower bound is seen to be almost linear. Finally, in the same Figure we

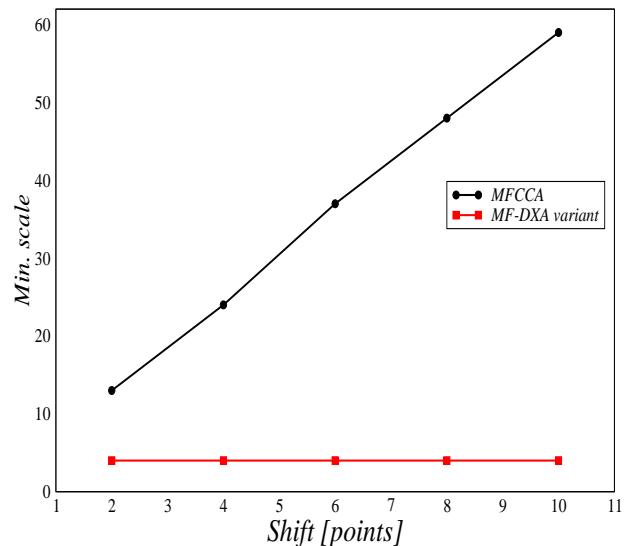


FIG. 8: Lower bound of the scaling regime that can be used in the calculation of  $\lambda_q$  as a function of the shift between the two MSM with  $m_0 = 1.2$  generated identical time series. The circles and the squares refer to calculations performed by means of MFCCA algorithm and a variant of MF-DXA procedure, respectively.

present the result of an analogous analysis but performed by means of the popular variant of MF-DXA procedure, that, in order to resolve the sign problem, makes use of the absolute values of the fluctuation functions [24–26]. In this case, the procedure is seen not to be sensitive to this type of surrogate and, thus, evidently generates spurious cross-correlations.

### C. Example of stock market data

As the final example of utility of the MFCCA method, we present an analysis of empirical data coming from the German stock exchange. As multifractal analysis of financial data is one of the most informative methods of investigating such complex systems [2, 15, 17, 32], we believe that MFCCA will be particularly useful in this field. We consider logarithmic price increments  $g(i)$  and linear time increments  $\Delta t(i)$  representing dynamics of a sample German stocks - E.ON (EOA) and Deutsche Bank (DBK) (from the same database as used before [2]) being part of the DAX30 index. These quantities are obtained according to the formulas:

$$g(i) = \ln(p(i+1)) - \ln(p(i)), \quad (17)$$

$$\Delta t(i) = t(i+1) - t(i), \quad (18)$$

where  $p(i), i = 1, \dots, N$  is a time series of price quotes taken in discrete transaction time  $t(i)$ . As we have shown in our earlier paper [2], both  $g(i)$  and  $\Delta t(i)$  are processes with self-similar structure and could be analyzed by the

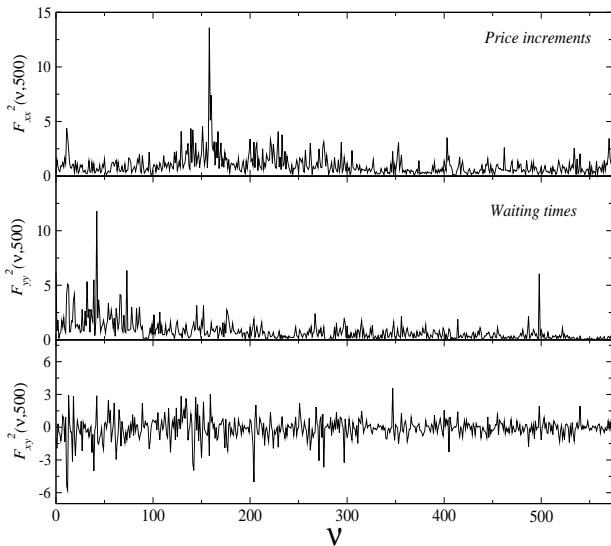


FIG. 9: Top and middle: detrended variance functions  $F_{xx}^2(\nu, 500)$  and  $F_{yy}^2(\nu, 500)$  calculated for time series of price increments and waiting times of E.ON (EOA) stock, respectively. Bottom: detrended cross-covariance function  $F_{xy}^2(\nu, 500)$  calculated for the same data. The calculations were carried out for segments of length of 500 points.

multifractal methods. Our analysis is performed on time series comprising the period between Nov. 28, 1997 and Dec. 31, 1999. The time series consists of  $T = 294862$  and  $T = 497513$  points for EOA and DBK, respectively. Therefore, the time series are long enough to bring statistically significant results.

In Fig. 9, we show one of the first steps of our algorithm, i.e., the detrended cross-covariance function  $F_{xy}^2(\nu, 500)$  (for the scale  $s = 500$ ) as a function of the box number  $\nu$  (Eq. (2)). For comparison, in the same Fig. 9, we depicted the detrended variance function  $F_{xx}^2(\nu, 500)$  and  $F_{yy}^2(\nu, 500)$  (obtained from MFDFA) calculated for individual time series of price increments and waiting times, respectively. It is easy to notice that the detrended variance calculated for individual time series takes only positive values, whereas the detrended cross-correlation fluctuation function takes both negative and positive values. Thus, in a cross-correlative analysis, amplification (or suppression) of fluctuations of  $F_{xy}^2(\nu, s)$  should take into account sign of the fluctuations. Otherwise, complex numbers associated with power (with some exponents) of negative fluctuations may appear in the  $q$ th order covariance function. This problem does not affect the fractal analysis of individual time series, because the detrended variance function is only positive.

In order to characterize the cross-correlations in the situation as above, the function  $F_{xy}^q(s)$  defined by Eq. (3) can be calculated. It turns out, however, that the scaling relation of  $F_{xy}^q(s)$  can only be observed for positive  $q$ 's. For the negative ones,  $F_{xy}^q$  fluctuates around zero and Eq. (5) is not satisfied. In Fig. 10 (top), the functions  $F_{xy}$  for EOA and DBK are displayed for positive values

of  $q$ . On each of these graphs, the top and the bottom lines refer to  $q = 4$  and  $q = 1$ , respectively. At first glance, we can notice that the slope coefficients of  $F_{xy}^q(s)$  depend clearly on  $q$ , especially for EOA. This is a signature of multiscaling of the underlying cross-correlation. The calculated  $\lambda_q$  and  $h_{xy}(q)$  are shown in the bottom panels of Fig. 10. It is clearly visible that, for EOA, both functions converge to each other for large values of  $q$ , while, for smaller ones,  $\lambda_q$  is significantly larger than  $h_{xy}(q)$ . These results imply that the scaling properties of the cross-covariance function strongly depend on the considered time span and they cannot be fully quantified by a unique exponent  $\lambda_q$ . Moreover, based on our results for MSM model, we can infer that the analyzed processes are ruled by the similar fractal dynamics only in periods with relatively large  $F_{xy}^2$  (associated with large  $q$ ). For smaller  $q$ 's, the difference between  $\lambda_q$  and  $h_{xy}(q)$  is more evident, which suggests that dynamics of these processes is significantly different, but still cross-correlative. It is worth to mention that large values of  $F_{xy}^2$  can be a consequence of cross-correlation both in the signs and the amplitudes of the signals. However, the waiting times are unsigned and the price increments are signed, but the sign is uncorrelated. This means that, in our case, the amplitude of  $F_{xy}^2$  is only a result of the cross-correlation of the observed amplitude. The strong cross-correlation of volatility (modulus of time series) is confirmed by Fig.11, where the cross-correlation function for the waiting times and absolute values of the price increments is depicted. Therefore, we conclude that large fluctuations are much more strongly cross-correlated than the smaller ones. Complexity of the multifractal cross-correlation is expressed by the wide range of  $\lambda_q$ , which is approximately 0.32 in this case.

For DBK, the behavior of  $\lambda_q$  is slightly different and the difference between  $h_{xy}(q)$  and  $\lambda_q$  is substantial both for small and for large values of  $q$  (Fig. 10, right panel). Also  $\Delta\lambda_q$  for DBK is smaller than in the case of EOA and takes a value of 0.22. This suggest that although structure of the cross-correlation between the inter-transaction times and the price increments for DBK is multifractal, its heterogeneity is poorer than in the case of EOA. Moreover, similarity between the fractal dynamics of large fluctuations is not so evident than in the former case. These results are also confirmed by Fig. 11, where a difference between the strength of volatility cross-correlations for both considered stocks is easily visible.

Presented results indicate that the multifractal cross-correlation characterizes only relatively large fluctuations of the processes under study. Smaller fluctuations that are filtered out by  $q < 1$ , from the perspective of our method, may be considered mutually independent.

Finally we wish to mention - but without showing the results explicitly in order not to confuse the reader - that taking absolute values of the fluctuation functions to get rid of the sign problem as recently often done in the literature [24–26] in the present financial data case results

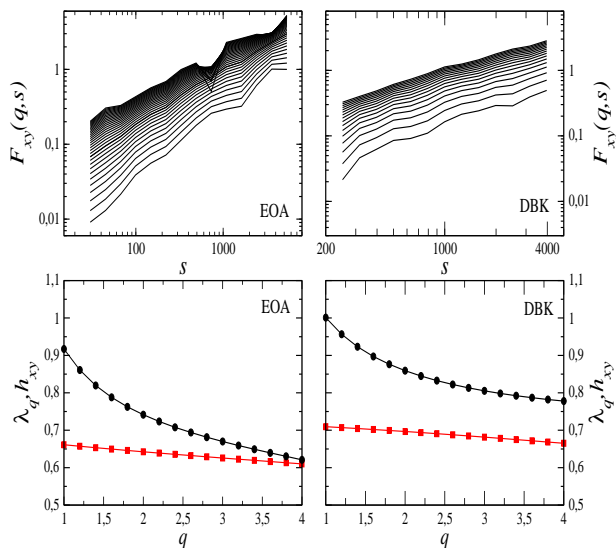


FIG. 10:  $F_{xy}^q(s)$  (top),  $\lambda_q$ , and  $h_{xy}(q)$  (bottom) calculated for time series of price increments and waiting times of E.ON (EOA) and Deutsche Bank s(DBK).  $F_{xy}^q(q, s)$  are estimated only for  $1 < q < 4$ . Black circles and red squares in the bottom panels refer to  $\lambda_q$  and the average of the generalized fractal exponents  $h_{xy}(q)$ , respectively.

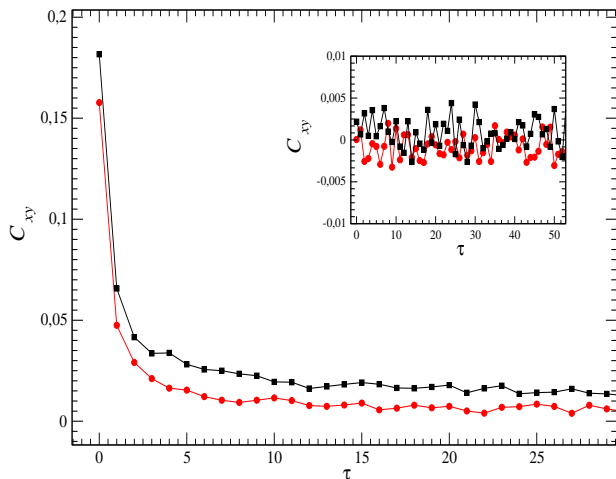


FIG. 11: Cross-correlation function  $C_{xy}(\tau) = |x_{i+\tau}| |y_i|$  corresponding to modulus of price increments and transaction times of EOA (black squares) and DBK (red circles). Inset: the same function but calculated for randomly shuffled data.

in a convincing multifractal scaling for all values of  $q$ -parameter. Furthermore, similarly as for the MSM model the so determined  $\lambda_q$  equals  $h_{xy}(q)$ . This way one, however, does not extract genuine correlations but only measures the averaged multifractal properties of individual time series.

#### IV. SUMMARY AND CONCLUSIONS

We proposed a modified algorithm that quantitatively describes multifractal aspects of cross-correlations among model and real-word time series and is free of several limitations that the other existing algorithms suffer from. We showed that outcomes of our algorithm provided more complete information about the structure of cross-correlations than a single exponent did. Moreover, the spectrum of  $\lambda_q$  combined with the average of the Hölder exponents  $h_{xy}(q)$  calculated for each time series separately contains information about similarity of their fractal structure. For example, in the case of artificially generated signals, the larger is the difference between  $\lambda_q$  and  $h_{xy}(q)$ , the more different are the considered (multi)fractals. These model results are crucial for a proper interpretation of the multifractal cross-correlations obtained for empirical data. As an example, we investigated a relation between sample pair of financial time series representing waiting times and price increments and found that these signals were multifractally cross-correlated but only for relatively large fluctuations, whereas the small ones could be considered mutually independent.

#### V. ACKNOWLEDGEMENTS

The calculations were done at the Academic Computer Centre CYFRONET AGH, Kraków, Poland (Zeus Super-computer) using Matlab environment.

[1] J. Kwapien and S. Drozd, Phys. Rep **515**, 115-226 (2012).  
 [2] P. Oświęcimka et al., Physica A (347), 626 (2005).  
 [3] S. Drozd, et al., EPL **88**, 60003, (2009).  
 [4] J.W. Kantelhardt et al., Physica A **316**, 87 (2002).  
 [5] D. Grech and Z. Mazur, Phys. Rev. E **87**, 052809 (2013).  
 [6] J.F. Muzy, et al., Int. J. Bifurc. Chaos **4**, 245 (1994).  
 [7] P. Oświęcimka, J. Kwapien, and S. Drozd, Phys. Rev. E **74**, 016103 (2006).

[8] J.F. Muzy, et al., EPL **82**, 60007 (2008).  
 [9] A.R. Subramaniam, I.A. Gruzberg, and A.W.W. Ludwig, Phys. Rev. B **78**, 245105 (2008).  
 [10] P.Ch. Ivanov, et al., Nature **399**, 461-465 (1999).  
 [11] D. Makowiec, et al., Physica A **388** 3486-3502 (2009).  
 [12] A. Rosas, E. Nogueira Jr., and J.F. Fontanari, Phys. Rev. E **66**, 061906 (2002).  
 [13] H.E. Stanley and P. Meakin, Nature **335**, 405-409 (1988).  
 [14] V.V. Udovichenko and P.E. Strizhak, Theoretical and



- Experimental Chemistry **38**,259-262 (2002).
- [15] S. Drożdż, et al., New J. Phys. **12** 105003 (2010).
  - [16] P. Oświęcimka, et al., Acta Phys Pol. A **114**, 547 (2008).
  - [17] W.-X Zhou, EPL **88**, 28004 (2009).
  - [18] G.R. Jafari, et al., J. Stat. Mech., P04012 (2007).
  - [19] P. Oświęcimka, et al., arXiv:1106.2902 (2011).
  - [20] B. Podobnik and H.E. Stanley, Phys. Rev. Lett. **100**,084102 (2008).
  - [21] B. Podobnik, et al., Proc. Natl. Acad. Sci. USA **106**, 22079 (2009).
  - [22] J.W. Kantelhardt, et al., Physica A **295**, 441-454 (2001).
  - [23] W.-X Zhou, Phys. Rev. E **77**,066211 (2008).
  - [24] L.-Y. He and S.-P. Chen, Physica A, **390**, 297-308 (2011).
  - [25] Z. Li and X. Lu, Physica A, **391**, 3930-3941 (2012).
  - [26] G.-J. Wang and C. Xie, Acta Phys. Pol. B **43** 2021 (2012).
  - [27] J. Hosking, Biometrika **68**, 165 (1981).
  - [28] E. L. Siqueira Jr. et al., Physica A **389**, 2739-2743 (2010).
  - [29] S. Shadhoo and G.R. Jafari, Eur. Phys. J. B **72**, 679-683 (2009).
  - [30] R. Liu et al. Physica A **383**, 35-42 (2007).
  - [31] R. Liu et al. Kiel Working Paper No. 1427 (2008).
  - [32] J. Kwapien et al. Physica A **350**, 466 (2005).